STRUCTURAL DESIGN OF FLOODWAYS UNDER EXTREME FLOOD LOADING

ABSTRACT

Purpose:

Current methods for floodway design are predominately based on hydrological and hydraulic design principles. This article investigates a finite element methods approach for the inclusion of a simplified structural design method into floodway design procedures.

Design/methodology/approach:

This research utilises a three-dimensional finite element method to investigate numerically the different parameters, geometric configurations and loading combinations which cause floodway vulnerability during extreme flood events. The worst-case loading scenario is then utilised as the basis for design from which several structural design charts are deduced. These charts enable design bending moments and shear forces to be extracted and the cross-sectional area of steel and concrete to be designed in accordance with the relevant design codes for strength, serviceability and durability.

Findings:

It was discovered that the analysed floodway structure is most vulnerable when impacted by a 4-tonne boulder, a 900 mm cut-off wall depth and with no downstream rock protection. Design charts were created forming a simplified structural design process to strengthen the current hydraulic design approach provided in current floodway design guidelines. This developed procedure is demonstrated through application with an example floodway structural design.

Originality/value:

The deduced structural design process will ensure floodway structures have adequate structural resilience, aiding in reduced maintenance and periods of unserviceability in the wake of extreme flood events.

Keywords: Floods; Floodways; Infrastructure; Bridge failure; Resilience; Impact load
Article Classification: Research Paper

1. INTRODUCTION

Resilient road networks are essential for the safety and wealth of communities worldwide (Pregnolato et al., 2017). Floodways (Figure 1a) can be described as road infrastructure utilised in road design to facilitate the safe crossing of water courses during low flow flood events (Wahalathantri et al., 2018). During such events the floodway structure is designed to be overtopped in a controlled and uniform manner dissipating flow concentration, thus reducing the likelihood of downstream scour and erosion. If floodwaters increase above safe crossing limits of 300 mm then vehicular access is precluded (Main Roads Western Australia, 2006). The incorporation of floodways offers a cost-effective solution when considering the cost benefit for use in rural road networks that do not service sufficient people to warrant large and expensive structures such as culverts and bridges (Lumor et al., 2017).

Figure (1)

The frequency of flood events has increased, jeopardizing the resilience of the built environment (Kimura et al., 2017). Flood related hydrological disasters have the highest occurrence rate of all-natural disasters worldwide causing significant economic loss (Du et al., 2019). Road structures located within waterways such as floodways, culverts and bridges are assets that frequently sustain damage and/or catastrophic failure as a direct result of increased flood waters (BNHCRC, 2015). These road structures serve a vital role in post disaster recovery and need to be designed in a manner that allows them to remain open and serviceable both during and after extreme flood events (Hung & Yau, 2014). To achieve a flood-resilient design, time of exposure to flood events and/or minimizing vulnerabilities through incorporating proper structural mitigation measures is crucial (Chowdhooree & Islam, 2018).

Australia relies heavily on floodway structures to service its vast rural road network. Studies into numerous regional councils throughout Australia have reported repeat structural damage and consistent failure mechanisms. These studies include GHD (2012) who investigated damage to floodways in five different South Australian regional councils, Wahalathantri et al., (2015) who investigated damaged structures in Southern Queensland and the authors of this paper who visited damaged floodway sites in Lockyer Valley Regional Council and Albury City Council as shown in Figures 1a and b.

In January 2011 the State of Queensland experienced **widespread** flooding which again repeated in 2013. These flood events caused rapid run-off as a result of heavy rainfall inundating 62% of the state of Queensland (QLD) and caused a reported $234 million in damage to the built environment (Setunge et al., 2014). More specifically, the Lockyer Valley region in QLD, the focus of this research exceeded an average exceedance probability (AEP) of 1 in 200, took 19 lives and out of 330 floodways in the region, 77 catastrophically failed and 115 sustained direct damage (Wahalathantri et al., 2015). These flood events highlighted the importance of the floodway design process and the need to investigate the critical design parameters, failure mechanisms and integrity of floodway structures to enhance the resilience of the rural road network (Wahalathantri et al., 2018).

A team of researchers [BNHCRC, 2015; Wahalathantri et al., 2015] undertook research into the most common failure modes of damaged floodways in the Lockyer Valley Region. This research discovered that the most common mode of failure was caused by direct impact from floating debris such as logs and boulders being conveyed by the increased flood water. In addition, erosion was

present at many of the damaged floodway sites indicated by scouring in the immediate upstream and downstream rock protection zones (Figure 1b). In some severe cases undermining of the floodway superstructure was also present. GHD (2012) reported that the presence of downstream erosion at a floodway site, if left unrepaired has the potential to form an erosion head cut. This erosion head cut can move upstream at variable rates based on the creek beds strata characteristics and may result in structural failure if it contacts the floodway.

As a direct result of the widespread damage sustained by floodways in 2011, the Lockyer Valley Regional Council investigated and implemented several revisions to the geometric features used within their standard engineering floodway designs. These revisions are summarised as follows;

- Inclusion of a cut-off wall to the entire perimeter of the floodway. Initially Lockyer Valley Regional Council constructed floodways with cut-off walls at the upstream and downstream extents only, however in recent years they have begun including the cut-off wall to the entire floodway perimeter to prevent ground water flowing through the underlying granular road pavement. This arrangement also provides further assurance against undermining of the superstructure.
- Trialing cut-off wall depths, defined as treatment options by Lockyer Valley Regional Council, of 900 mm and 1100 mm as shown in Figure 2. Lockyer Valley Regional Council currently selects cut-off wall depth based on the proposed sites average stream velocity. It is anticipated that the cut-off wall will provide increased lateral resistance as a result of the greater surface area present. Further, the increased cut-off wall depth will provide greater structural resilience if a downstream erosion head cut contacts the floodway superstructure.

Figure (2)

Current design guidelines **for** floodway design **are** based predominately upon hydrological and hydraulic design principles [Queensland Department of Transport and Main Roads, 2010; Main Roads Western Australia, 2006; Austroads Ltd, 2013; US Army Corps of Engineers Afghanistan Engineer District, 2009; Lohnes et al., 2001]. **As a result of this, current design practises tend to neglect the forces that floodways are exposed to, yet expected to withstand, during extreme flood events. These hydrological and hydraulic design principles utilise the Empirical Broad-Crested Weir formula and Mannings formula for raised and flush floodway structures respectively.** These formulas contain a number of assumptions including; the water course is of an open prismatic and uniform channel and **through the application of a mean velocity in Manning's equation inaccuracies are introduced as often the velocity is lower at the deeper sections within a creek and subsequently higher at the edges and mid-section, which results in higher stresses** (BNHCRC, 2015a). The studies conducted by Wahalathantri et al. (2018) also concluded that floodways often exist in complex surroundings that include horizontal and vertical bends. Due to these complexities, assumptions **utilised** by the current **hydraulic focused** design guidelines **often create outcomes which are less than optimal**.

2. RESEARCH SIGNIFICANCE

This research, through the undertaking of a Finite Element Methods approach expands on the authors conference paper titled *"Floodway Design Process Revisited"* (Greene et al., 2019) to deduce

what causes a standard engineering floodway type to be most vulnerable, while acting in a frequently submerged state. Utilising this state of vulnerability as the basis of design, ultimate design bending moments and shear forces can be determined and structural design charts deduced. These design charts enable design bending moments and shear forces to be extracted **and** steel reinforcement **in** concrete to be designed in accordance with the relevant design codes for strength, serviceability and durability. This simplified structural design method incorporated with the current design guidelines will enable local government authorities to design resilient floodway structures with confidence.

3. METHODOLOGY

Three-dimensional finite element modelling, and subsequent analysis was conducted using finite element computational software, Strand7 (Strand7, 2019). Finite Element Methods is widely adopted and **utilised** in a variety of numerical modelling applications and structural problem solving. Model development methods and test variables used to construct the three-dimensional floodway model are outlined in this section.

'*Concrete Floodway Type-2'*, a commonly implemented standard engineering floodway type from the Lockyer Valley Region in Queensland was selected for modeling as shown in Figure 3. The Type-2 floodway is often implemented in creeks of relatively flat grade and where a hydraulic control is not required to be imparted on the creek to facilitate safe vehicular crossing conditions.

Figure (3)

3.1 Model Development

Details of modelling techniques, criterions and selected parameters utilised in this research are summarised as follows:

- *Element types and criterions:* Four node tetrahedra Strand7 brick elements were used to construct the three-dimensional model. Mohr-coulomb yield criterion, a commonly implemented failure model for geotechnical materials was used to analyse the non-linear behavior of soil materials where behavior is governed by cohesion and internal friction angle (Jiang, 2018). Max Stress yield criterion was assigned to concrete brick elements and defines failure when stress components exceed yield strength in either compression or tension (Feng, Malingam & Irulappasamy, 2019). As this criterion is stress dependent a stress versus strain curve was defined in Strand7 to represent the nonlinear elastic behaviour of concrete in both compression and tension.
- *Boundary conditions:* Boundary conditions were assigned to the outer model extents to imitate in-situ support conditions of a floodway situated in infinite length and depth of natural adjoining strata. That is, the outer faces were assigned roller support conditions and the bottom face rigid support conditions. Roller supports permitted movement in the vertical axis yet precluded movement in the horizontal axis (normal to the vertical plane). Rigid supports are fixed against displacement and rotation.
- *Mesh and model refinement:* To determine the influence of the restraints and mesh size the extent of adjoining natural earth and mesh density was iteratively increased until a converged numerical solution resulted. This was found to be achieved by a model consisting of 26,244 nodes and 23,584 brick elements with a profile length of 26.4 m, width of 21.5 m and a depth

of 20.9 m as shown in Figure 4. It should be noted that for the model depth to converge, Strand7 tool *'Auto Assign Insitu Stress'* was utilised.

Figure (4)

- *Water level:* To model the change in water level for soil materials, fluid level was set in respect to the coordinate value of the Global Axis corresponding to the gravity direction. This required the definition of multiple element property types for each water level, along with the approximation of the actual water level profile into a series of constant water levels for advanced and/or irregular shaped elements. On completion, in-situ stresses were calculated and the vertical in-situ stress profile under self-weight was observed for any variance.
- *Concrete-soil interface:* It was concluded that omitting contact interface was satisfactory for flow velocities less than or equal to 8 m/s as loading was calculated to be well below the maximum frictional force, refer Sub-Section 2.2 for further details.
- *Mechanical properties:* Material mechanical properties assigned to the model are defined in Table 1. Rock protection was assumed to be made up of individual loose packed rocks (lower modulus and density) which behave as a soil material defined by Mohr-Coulomb criterion i.e. a homogeneous, elastic-plastic and isotropic material, a criterion frequently utilised in practice to model geotechnical material failure (Jiang, 2018). Steel reinforcement in concrete was neglected, allowing tensile forces apparent to be determined and reinforcement designed accordingly in the structural design method presented.

Table (1)

3.2 Verification

Due to the complexity of the full-size model and the use of a nonlinear analysis, a verification model representing a component of the augmented model was utilised to provide model confidence. This verification model was used to validate modelling techniques, material criterion, convergence controls and model response, with errors identified, analysed and omitted.

- *Elastic response:* Hooke's Law, is a common engineering model used to approximate a material stress-strain relationship assuming elastic properties where force and displacement are proportional (Johnson, 2006). This relationship can be represented by equation 1 and was used to resolve vertical displacement for each of the layered elastic materials in the verification model. By comparing total elastic displacement calculated by Hooke's law to that of the linear static solver output, discrepancies in the model's response could be determined.

$$\delta = \frac{PL}{EA} \quad (1)$$

Where: δ is vertical displacement in [m], P is the applied force in [N], L is length in [m], E is the Modulus of Elasticity in [MPa] and A is the area in [m^2].

- *Visual response:* Visual inspection of the magnitude and shape of deformation was checked to ensure uniformity and that realistic results were being obtained for each verification case considered.

- *Mohr-Coulomb response with concrete-soil interface:* The vertical cross-section of the floodway consisted of layered materials with varying frictional interfaces. The most critical interface existed between the concrete apron and the compacted gravel sub-base. The effect of contact was analysed using the Coulomb friction/Elliptical Plastic model after inducing a small gap between the layers and linking the two regular meshes so that they are in immediate contact. Further, contact behaves non-linearly and so the nonlinear static solver within Strand7 was selected. To assist in obtaining a converged result, load stepping was used in the nonlinear static solver to incrementally apply loading and to prevent over-penetration during the initial load application.

  Two friction coefficients, 0.55 and 0.99 were selected to represent a case with and without contact respectively. The limiting load (maximum frictional force) was calculated using the static friction formula in equation 2 for the two friction coefficients.

  $$F = \mu N \qquad (2)$$

  Where: *F* is force in [N], μ friction coefficient (unitless) and *N* is the normal force in [N].

  For a friction coefficient of 0.99 and all loads well below the limiting load of 0.1049 MPa displacement results with contact remained very similar to the displacement results without contact.

  Table 2 shows the results obtained for a friction coefficient of 0.55. Results for loadings well below the limiting load of 0.0582 MPa remained similar for both with and without contact. As the loading approached the limiting load, results began to diverge indicating that the concrete was on the verge of displacement. When the load exceeded the maximum frictional force, the solver could no longer converge indicating that the concrete had displaced.

Table (2)

It was concluded to omit contact elements since the loads being modelled remain well below the limiting load and therefore no significant discrepancy in results will occur.

3.3 Test Variables and Loading Combinations

A range of variables were selected for use in the parametric analysis. The values used for these variables were consistent with those recorded during the 2011 flood event in the Lockyer Valley Region and the design considerations implemented by the Lockyer Valley Regional Council.

- Flow depth intervals consisting of 0, 1 and 2 m above the road surface. For vehicular loading this was limited to 0.3 m corresponding to the maximum permissible crossing depth specified by Austroads Ltd (2013).
- Upstream velocities of up to 8 m/s;
- Varying boulder mass between 2 and 4 tonnes;
- Varying cut-off wall depth between 900 and 1100 mm;
- Varying adjacent soil types; and

- Varying downstream rock protection extent between; full protection, no protection and no protection or soil adjacent the downstream cut-off wall. The latter simulating a downstream head cut contacting the floodway superstructure.

Three different loading combinations were selected for analysis as follows;

A. Hydrostatic loading:

Hydrostatic pressure was assumed to behave in accordance with hydrostatic fluid force theory, that is normal to the surface of the object and in a linear manner where the mediums density is directly proportional to height as shown in equation 3.

$$P = \rho g h \quad (3)$$

Where: P is hydrostatic pressure in [Pa], ρ is the mediums density in [kg/m^3], g is gravity in [m/s^2] and h is height of fluid in [m].

B. Boulder impact and hydrostatic loading:

Boulder impact loading was calculated by applying a factor of 0.5 to the log impact formula provided in AS 5100.2:2017, *'Bridge Design, Design Loads'* (Australian Standards 2017). The 0.5 factor was considered appropriate as boulders are not suspended articles like logs, rather they remain in contact with the creek bed.

$$F_{log} = 0.5(mV^2/2d) \quad (4)$$

Where: F_{log} is force in [N], m is the objects mass in [kg], V is the objects velocity in [m/s] and d is the stopping distance in [m].

Velocities required to propagate the movement of a 4-tonne boulder were derived from Main Roads Western Australia (2006) tables for rock protection scour velocities.

C. Vehicular, debris and hydrostatic loading:

For vehicular loading a maximum permissible crossing depth of 0.3 m was considered as specified by Austroads Ltd (2013).

Traffic loads were applied in a static state and approximated the effects induced by moving traffic and stationary queues in accordance with AS5100.1 (Australian Standards 2017). Due to the rural setting, a W80 wheel load corresponding to an 80 kN load uniformly distributed over an area of 400 mm x 250 mm was considered appropriate.

Debris loading was calculated using equation 5 based on AS 5100.2:2017 (Australian Standards 2017).

$$F_{deb} = 0.5 C_d V_u^2 A_{deb} \quad (5)$$

Where: C_d is the coefficient of debris.

Drag force was omitted based on the negligible effect (Cummings, 2018). A load factor of 1.3 was applied to all design loads from AS5100.2:2017 to satisfy ultimate limit state (ULS) conditions (Australian Standards 2017). Hydrostatic force being an exception which had a load factor of 1.5 applied based on AS1170.1 (Australian Standards 2002).

4. RESULTS AND DISCUSSION

4.1 Simulation of Loading Combinations

4.1.1 Load Combination A - Hydrostatic Loading

Combination A considers the floodway, situated level with the creek bed and with no surface area acting perpendicular to the direction of flow. Lateral loadings that increase proportionally to velocity such as debris and impact are therefore omitted; however, a range of hydrostatic loads are applicable. This case was selected in response to the findings in GHD (2012), which reported that road authorities were removing damaged floodway structures and vertically realigning them flush with the creek bed after observing minimum damage post flood events.

Figure (5)

Figure 5a shows vertical displacement increased downwards linearly as flow depth increased. This resulted since hydrostatic loading is proportional to flow depth. Similarly, Von Mises stress also increased proportionally to flow depth (Figure 5b). The maximum vertical displacement and Von Mises stress of 2.15 mm and 1.04 MPa respectively occurred at a flow depth of 2m.

4.1.2 Load Combination B - Boulder Impact and Hydrostatic Loading

Combination B considered a 2-tonne boulder impacting the floodway. In this combination the floodway was modelled in a damaged state with reduced upstream rock protection causing the upstream leading edge to protrude and act perpendicular to the direction of flow.

Displacement in the direction of flow increased proportionally to flow velocity corresponding to an increase in impact loading (Figure 6a). Horizontal displacement decreased as flow depth increased due to the increase in frictional forces present. The highest horizontal displacement was 0.908 mm which occurred at 1 m and 8 m/s flow depth and velocity respectively.

Flow depth influenced the resulting Von Mises stress up until approximately 4 m/s, this trend was more evident as flow depth increased as illustrated in Figure 6b by the change in direction at approximately 4 m/s for the 2m flow depth. Once flow velocity increased past 4 m/s, impact loading was the most dominate force resulting in the three flow depths increasing exponentially with flow velocity. The highest stress of 2.423 MPa occurred when flow velocity and flow depth were both at a maximum corresponding to the largest impact force.

Figure (6)

4.1.3 Load Combination C – Vehicular, Debris & Hydrostatic Loading

Combination C also considered the floodway type in a damaged state and therefore conducive to lateral loads such as debris loading. In addition, vertical vehicular and hydrostatic loading were applied up to the maximum permissible crossing depth of 0.3 m (Austroads Ltd, 2013). Traffic loads were applied as a static loading which approximated the effects induced by moving traffic and stationary queues in accordance with AS5100.1 (Australian Standards 2017).

Displacement in the horizontal direction (direction of flow) increased proportionally to flow velocity which corresponded to an increase in debris loading (Figure 7a). Horizontal displacement also decreased as hydrostatic loading increased due to an increase in frictional force. The highest

horizontal displacement of 0.5 mm occurred when flow depth was at a minimum and flow velocity was at a maximum.

Figure (7)

Von Mises stress increased exponentially due to debris accumulation being proportional to both flow velocity and depth (Figure 7b). The highest stress of 1.93 MPa occurred when flow velocity and depth were at a maximum.

4.1.4 Discussion

Load Combination A produced the lowest stress and displacement results for the three loading combinations considered. This combination remains applicable if no surface acts perpendicular to the watercourse, resulting in a very efficient floodway design where stress and vertical displacement results are directly proportional to flow depth. This further supports GHD (2012) who observed road authorities removing damaged floodway structures and realigning them flush with the creek bed.

Reviewing the three loading combinations, Combination B consistently produced the highest stress and displacement results and was therefore adopted for further detailed parametric analysis of design parameters.

4.2 Simulation of Varying Design Parameters

Different design features, geometry and load configurations consistent with that currently being implemented by the Lockyer Valley Regional Council were investigated. These parameters included impact loading magnitude, cut-off wall depth, extent of downstream rock protection and different adjoining soil types.

4.2.1 Boulder mass

Boulder mass was increased from 2 to 4-tonnes, a load equivalent in magnitude to a 2-tonne floating log as considered in AS 5100.2:2017 (Australian Standards 2017). As flow velocity increased, horizontal displacement in the 4-tonne boulder case diverged and was 61.07% greater than the 2-tonne boulder when flow velocity was at a maximum (Figure 8a). Von Mises stresses also followed a similar diverging trend with stresses 52.98% greater than the 2-tonne boulder case when flow velocity was at maximum (Figure 8b).

Figure (8)

4.2.2 Cut-off Wall Configuration

Investigation into different length cut-off walls defined as *'treatment* options' provided comparison between a 1100 mm cut-off wall and the commonly utilised 900 mm cut-off wall depth. For the 1100mm cut-off wall depth both maximum horizontal and vertical deflection were reduced by 1.06% and 3.94% respectively (Figure 9a). This reduction in deflection is a result of the greater distribution of forces to the adjoining soil due to the increased surface area, subsequently increasing stabilising moment. Similarly, Von Mises stresses slightly decreased by 0.781% (Figure 9b).

Figure (9)

4.2.3 Downstream Rock Protection

Erosion of downstream rock protection was modelled by incrementally reducing the depth of rock protection and soil extent adjacent the downstream cut-off wall. This was conducted over three increments which included; full downstream rock protection, no downstream rock protection and no downstream rock protection or natural soil adjacent the downstream cut-off wall.

For velocities below approximately 7.5 m/s horizontal displacement decreased as material adjacent to the cut-off wall decreased (eroded). This subsequently caused water depth to increase creating **a larger** opposing hydrostatic force. **At the highest velocity of 8 m/s,** the case with the largest resistance to lateral loading **reversed to** full downstream rock protection which resulted in 5.50% less horizontal deflection than the case with no downstream rock protection (Figure 10a). Von Mises stresses also converged at a flow velocity of approximately 3.5 m/s when impact loading became the most dominant force, after which a consistent increasing trend resulted (Figure 10b).

Figure (10)

4.2.4 Varying Soil Types

Three different soil properties (Table 3) were selected to reflect the different strata which floodways are frequently constructed within. *Soil 2*, a sandy soil resulted in the highest stress and displacement results out of all the soil types. Changing soil types was found to have a large influence on the variability of displacement and stress results. It was therefore decided to consider all soil types in the structural design procedure. This allows the structural design method to align with a range of insitu soil conditions specific to the floodway site locality.

Table (3)

4.2.5 Worst-Case Loading Scenario

The worst-case loading scenario occurs when the loading combination is at its most unfavourable and the design parameters that compromise floodway integrity are at their greatest. This state occurred when flow depth and flow velocity were at a maximum and for a 4-tonne boulder impact, no downstream rock protection and a 900 mm cut-off wall depth. This worst-case loading scenario formed the basis of the deduced structural design process detailed in subsequent sections. Mechanical properties of soil adjacent the floodway structure **was** considered independently.

4.3 Determining Design Bending Moments and Shear Forces

To extract bending moment and shear force from the worst-case loading scenario the following process was undertaken:

1. The ultimate limit state loading (1.2G + 1.5Q) AS1170 representing the worst-case loading scenario was applied to the three-dimensional (3D) floodway model and solved (Australian Standards AS1170: 2002);
2. Observation of the results highlighted areas containing the largest stress and displacement results. This was discovered to occur centrally and in the direction of flow (longitudinal). This was denoted as the line-of-action;
3. Along the line-of-action, displacements were recorded either side of the floodway;
4. The line-of-action was then reproduced by applying the recorded displacements to the nodes in a separate model containing a two-dimensional (2D) beam connected rigidly at joints. This 2D beam was of a nominal 1 m length in the z-direction and the cross section represented that of the 3D floodway model.
5. Solving the 2D beam model in Strand7 produced the resulting bending moments (M*) and shear force (V*) distribution. To confirm solution accuracy the Dx and Dy displacements from the 2D beam model were compared to that of the 3D cut-plane model; and
6. These steps were repeated for the three reported commonly encountered soil types and the maximum M* and V* were plotted as strength capacity charts for a range of different flow velocities and flow depths.

It was discovered that both positive and negative bending moments and shear forces act against the floodway superstructure (Figure 11). Further, these maximum positive and negative moments and shear forces are concentrated at the upstream and downstream cut-off wall and apron locations. These locations were subsequently selected for the development of strength capacity design charts representing the absolute moment and force acting on the structure.

Figure (11)

4.4 Strength Capacity Design Charts

This section presents a simplified structural design method for floodways based on the design bending moment and design shear force values deduced from the parametric finite element analysis. These values have been assembled into strength capacity design charts and are presented in figure 12 to 14. The design bending moment and shear force are absolute values for the floodway structure and are based on three commonly encountered soil types from the Lockyer Valley Region and for a range of different flow velocities and depths. Design of the floodway structural elements can then be conducted in reference to the relevant standards for concrete construction.

Figure (12)

Figure (13)

Figure (14)

Investigating the downward trend in the shear force design graphs it was found that hydrostatic loading (predominately a negative vertical load) and impact loading (positive horizontal load only) resulted in opposing load types and the trough of the design graph corresponded to the point at which they negated each other the greatest.

4.5 Structural Design Example

The following example illustrates the use of the strength capacity design charts to determine the reinforcement requirements of the floodway type. The aim of this design is to select the cross-sectional area of steel and concrete that satisfies the relevant countries code requirements for strength, serviceability and durability. For this design example, design will be in accordance with the requirements of Australian Standard AS3600:2009 (Australian Standards 2009).

4.5.1 Step 1: Determine design parameters

Design parameters include the specific site location, soil type, maximum flow velocity and depth. These factors are determined in conjunction with current floodway design guidelines, geotechnical testing and flood modelling software. For this example, the following parameters are assumed;

- Location: Lockyer Valley Regional Council (temperate environment);
- Soil Type: Soil Type 2;
- Maximum flow velocity: 7 m/s; and
- Maximum flow depth: 1.5 m.

Referencing the design charts for Soil Type 2 as presented in figure 13, the maximum bending moment and shear force can be extracted as 8.47 kN.m and 30.52 kN, respectively. Note linear interpolation can be used to determine intermediate values.

4.5.2 Step 2: Design for durability - Section 4, AS3600:2009

- Exposure classification is B1;
- Minimum compressive strength of 32 MPa satisfies durability requirements; and
- Minimum cover required is 40 mm, assuming standard formwork and compaction.

4.5.3 Step 3: Design for strength and serviceability in bending - Section 8.1, AS3600:2009

Assume the use of SL81 mesh to satisfy bending reinforcement requirements.

Figure (15)

$M^* = 8.47\ kN.m$, where M^* = design bending moment from design graphs

Calculating compressive force in concrete, F_c i.e. volume of the stress block;

$$F_c = (\alpha_2 f'_c)\ (\gamma d_n)\ b \qquad (6)$$

$$F_c = (0.85)(32)(0.826)(d_n)(1000)$$

$$F_c = 22467.2(d_n)$$

Calculating tensile forces in steel (assuming steel yields), F_t;

$$F_t = A_{st} f_{sy} \quad (7)$$
$$F_t = (363)(500)$$
$$F_t = 181{,}500$$

Equating F_t and F_c to determine the neutral axis depth;

$$F_t = F_c \quad (8)$$
$$d_n = 8.078\ mm$$

With d_n evaluated we can calculate the lever arm:

$$d = D - c - B/2 - \gamma \cdot d_n/2 \quad (9)$$
$$d = 250 - 40 - 8/2 - ((0.826)(8.078))/2$$
$$d = 202.66\ mm$$

Calculating moment capacity, M_u, gives;

$$M_u = F_t d = F_c d \quad (10)$$
$$M_u = (181{,}500 \times 10^{-3})(202.66)$$
$$M_u = 36.8\ kN.m$$

Checking if assumed bending reinforcement is satisfactory

$$\varphi M_u >= M^* \quad (11)$$

$(0.85)(36.8)\ kNm \geq 8.47\ kN.m$, therefore safe.

Outcome: ~~A~~adopt SL81 mesh reinforcement to both the inner and outer faces of the floodway to satisfy bending moment.

4.5.4 Step 4: Design for strength and serviceability in shear - section 8.2, AS3600:2009

$V^* = 30.52\ kN$, where V^* = design shear force at a cross section as determined from design charts.

Checking if shear reinforcement is required

$$V_{uc} = \beta_1 \beta_2 \beta_3 b_v d_o (A_{st} f'_c / b_v d_o)^{1/3} \quad (14)$$
$$V_{uc} = (1.537)(1)(1)(1000)(202.66)((363)(32)/(1000)(202.66))^{1/3}$$
$$V_{uc} = 119.46\ kN$$

$$\varphi V_{uc} \geq V^* \quad (15)$$

$0.5\varphi V_{uc}\ (0.5)(120.1\ kN) > V^*\ (30.52\ kN)$, therefore safe.

Outcome: Shear reinforcement is not required as the shear strength of 32 MPa concrete alone satisfies shear force requirements.

4.6 Integrated Design Procedure

The simplified structural design procedure is intended to be used in conjunction with the hydraulic design process detailed in the current design guidelines. The design procedure incorporating the structural design method is summarised in figure 16 and outlined as follows:

1. Select the point of waterway crossing based on the horizontal and vertical road alignment criteria and environmental factors stated in the design guidelines.
2. Derive the stage-discharge curve for the water course.
3. Calculate the optimum reduced level for the floodway deck (road surface) along with the expected discharge rate. This needs to be less than 300 mm and for a 20-year ARI event. As the Type-2 floodway is situated level with the creek bed (i.e. does not impart a hydraulic control on the stream), design discharge can simply be calculated using Mannings equation.
4. Determine design bending moment and design shear force based on the values obtained from the design charts illustrated in Figure 12 to 14. These values are based on the soil type encountered at the specific location along with the flow velocity and depth of the water course. Design of the floodway structural elements can then be undertaken to satisfy the relevant countries code requirements.
5. Select appropriate scour, pavement and embankment protection in accordance with the current floodway design guidelines.

Figure (16)

5. IMPLICATIONS FOR RESEARCH AND PRACTICE

This research incorporates a structural design process which addresses a gap in the current area of knowledge that focusses primarily on hydraulic design principles to deliver an improved and consistent design methodology. This structural design process considers the floodway in a submerged state and with external loadings equivalent to that experienced during an extreme flood event. As an outcome of this research, strength capacity charts containing design bending moment and shear force values for a single floodway type were derived providing designers with an accurate and expeditious method to determine the design forces apparent within the floodway structure under extreme flood loadings. Designers can then design structural elements in accordance with the relevant concrete design standards. Through the implementation of this design process it is expected that floodway structural resilience will be improved as a result of increased durability, serviceability and strength.

As floodways serve a critical purpose in the rural road network any improvement in structural design and integrity will ultimately increase rural community safety and resilience to extreme flood events. An increase in structural integrity and lowering of asset damage after a flood event will have a direct positive impact on local government expenditure, whilst minimising financial disruptions to the local communities through the prevention of access restrictions being imposed. By maintaining a safe access it will also enable quicker disaster response and recovery efforts following a major flooding event.

As this research considers only a single standard engineering floodway type which is currently implemented in the Lockyer Valley Regional Council the opportunity exists for alternative standard floodway types to be examined through the finite element method and parametric approach adopted in this research to provide a more widely adaptable approach.

Practical implementation of this design methodology would also allow performance to be quantified in real terms, based on exposure to different flood events. Opportunity also exists for

the application of this research and findings to be adopted to other small rural road structures such as culverts and bridges.

6. CONCLUSION

This research has investigated a finite element methods approach for the inclusion of structural analysis into current floodway design procedures. A parametric analysis was conducted for the standard engineering floodway type identifying areas of structural vulnerability and the worst-case loading scenario. This worst-case loading scenario was found to occur during the impact loading case, which incorporated a 4-tonne boulder impact, no downstream rock protection and a 900 mm cut-off wall depth. This configuration is consistent with the damage experienced to floodways during the Queensland floods of 2011 and 2013 as described by Wahalathantri (2018).

Based on this investigation several structural design charts were deduced. These charts provide the maximum absolute bending moment and shear force values from the worst-case loading scenario. These charts allow steel and concrete to be designed to satisfy the relevant countries code requirements for strength, serviceability and durability of concrete structures for this floodway type whilst under extreme flood loadings.

An integrated design method was developed to incorporate the structural design charts into the current hydraulic design procedures stated within floodway design guidelines. This process will ensure adequate structural resilience, aiding in reducing maintenance and periods of unserviceability in the wake of extreme flood events.

7. ACKNOWLEDGEMENTS

The authors would like to acknowledge the Lockyer Valley Regional Council for providing information relating to floodways and the support of the Commonwealth of Australia through the Cooperative Research Centre program; *Bushfire and Natural Hazard CRC* and the *Research Training Program (RTP) Scholarship*.

8. REFERENCES

Austroads Ltd (2013), *Guide to Road Design Part 5B: Drainage - Open Channels, Culverts and Floodway*, 1st edn, ARRB Group, Sydney.

Chowdhoor, I. and Islam, I. (2018), "Factors and actions for enhancing community flood resilience: an experience from a river-side settlement in Bangladesh", *International Journal of Disaster Resilience in the Built Environment*, Vol. 9 No. 2, pp. 153-169.

Cummings S 2015, *Modelling the Behaviour of Floodways Subjected to Flood Loadings*, undergraduate project, University of Southern Queensland, Toowoomba. Viewed 27/02/2019, https://eprints.usq.edu.au/29647/.

Du, W., Chen, N., Yuan, S., Wang, C., Huang, M. and Shen, H. (2019), "Sensor web - Enabled flood event process detection and instant service", *Environmental Modelling & Software*, Vol. 117, pp. 29-42.

Feng, N.L., Malingam, S.D. and Irulappasamy, S. (2019), "Bolted joint behavior of hybrid composites", *Woodhead Publishing Series in Composites Science and Engineering*, pp. 79-95.

GHD (2012), *"Report for Floodway Research Project"*, GHD PTY LTD, available at: http://www.lga.sa.gov.au/webdata/resources/project/Flood_Damage_Remediation_Approaches_Project_Output-1.pdf (accessed 29 March 2018).

Haddadi, H. and Rahimpour, M. (2012), "A discharge coefficient for a trapezoidal broad-crested side weir in subcritical flow", *Flow Measurement and Instrumentation*, Vol. 26, pp. 63-67.

Hung, C. and Yau, W. (2014), "Behavior of scoured bridge piers subjected to flood-induced loads", Engineering Structures, Vol. 80, pp. 241-250.

Greene, I., Lokuge, W. and Karunasena, W. (2019), "Floodway Design Process Revisited", in *Proceedings of the 25th Australasian Conference on Mechanics of Structures and Materials (ACMSM25) in Brisbane, Australia, 2018,* Springer, Singapore, pp. 995-1006.

Jiang, H. (2018), "Simple three-dimensional Mohr-Coulomb criteria for intact rocks", *International Journal of Rock Mechanics and Mining Sciences*, Vol. 105, pp. 145-159.

Kimura, N., Tai, A. and Hashimoto, A. (2017), "Flood caused by drift wood accumulation at a bridge", *International Journal of Disaster Resilience in the Built Environment*, Vol 8 No. 5, pp. 466-477.

Lohnes, R.A., Gu, R.R., McDonald, T. and Jha, M.K. (2001), "Low Water Stream Crossings: Design and Construction Recommendations", Iowa State University, Available at http://www.intrans.iastate.edu/reports/LWSC.pdf (accessed 13/04/2019).

Lumor, R.K., Ankrah, J.S., Bawa, S., Dadzie, E.A. and Osei, O. (2017), "Rehabilitation of timber bridges in Ghana with case studies of the Kaase Modular Timber Bridge", *Engineering Failure Analysis*, Vol. 82, pp. 514-524.

Main Roads Western Australia (2006), *Floodway Design Guide*, 6702-02-2230 edn, Main Roads Western Australia, Perth.

Obrzud, R.F. and Truty, A. (2018), "The Hardening Soil Model – A Practical Guidebook", Z_Soil.PC 100701 report, available at: http://www.zsoil.com/zsoil_manual_2018/Rep-HS-model.pdf (accessed 17 October 2019).

Pregnolato, M., Ford, A., Wilkinson, S. and Dawson, R. (2017), "The impact of flooding on road transport: A depth-disruption function", *Transportation Research Part D: Transport and Environment*, Vol. 55, pp. 67-81.

Queensland Department of Transport and Main Roads (2010), *Road Drainage Manual*, 1st edn, Queensland Department of Transport Main Roads, Brisbane.

Setunge, S., Lokuge, W., Mohseni, H. and Karunasena, W. (2014), "Vulnerability of road bridge infrastructure under extreme flood events", Paper presented at Australia Fire Authorities Council (AFAC) Conference, 2-5 September 2014, Wellington, New Zealand, available at: https://eprints.usq.edu.au/26242/ (accessed 05 July 2019)

Standards Australia (2002), "Structural Design Actions", AS1170.0-2002, Standards Australia, Sydney, available at: http://www.saiglobal.com/online/autologin.asp (accessed 05 March 2019).

Standards Australia (2017), "Bridge Design, Design Loads", Standards Australia, Sydney, Available at: http://www.saiglobal.com/online/autologin.asp (accessed 05 March 2019).

Standards Australia (2009), "Concrete Structures", Standards Australia, Sydney, Available at: http://www.saiglobal.com/online/autologin.asp (accessed 05 March 2019).

Strand7 (2018), *Strand7*, version 2.4.6, computer software, accessed 30 January 2019.

US Army Corps of Engineers Afghanistan Engineer District (2009), "AED Design Requirements: Culverts and Causeways", Version 1.3 ed.

Wahalathantri, B., Lokuge, W., Karunasena, W. and Setunge, S. (2018), "Quantitative assessment of flood discharges and floodway failures through cross-cultivation of advancement in knowledge and traditional practices", *International Journal of Disaster Resilience in the Built Environment*, Vol. 9 No. 4/5, pp. 435-456.

Wahalathantri, B.L., Lokuge, W., Karunasena, W. and Setunge, S. (2015), "Vulnerability of floodways under extreme flood Events", *Natural Hazards Review*, Vol. 17 No. 1.

(a)

(b)

Figure 1. (a) floodway structure incorporated in a rural road and (b) scour in the immediate downstream rock protection zone.

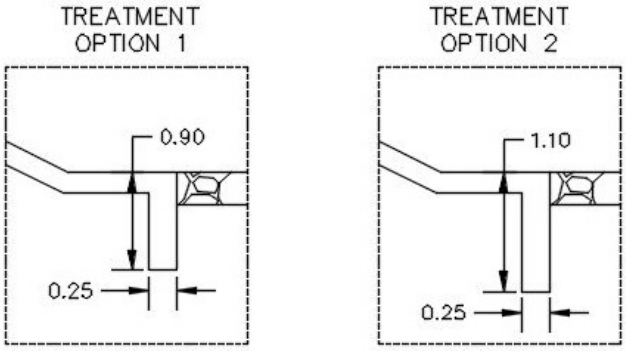

Figure 2. Schematics of treatment options applied to floodways in the Lockyer Valley Regional Council.

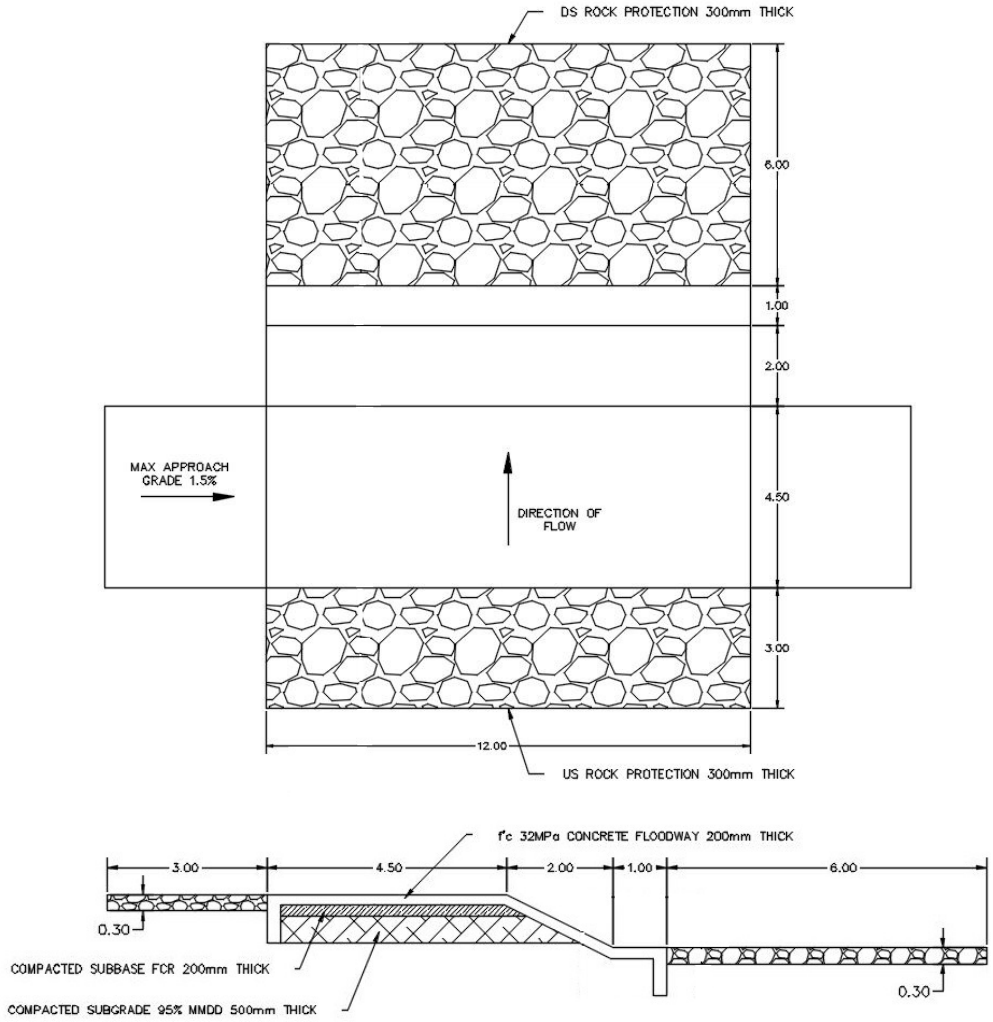

Figure 3. Plan and cross-section of the Type-2 floodway.

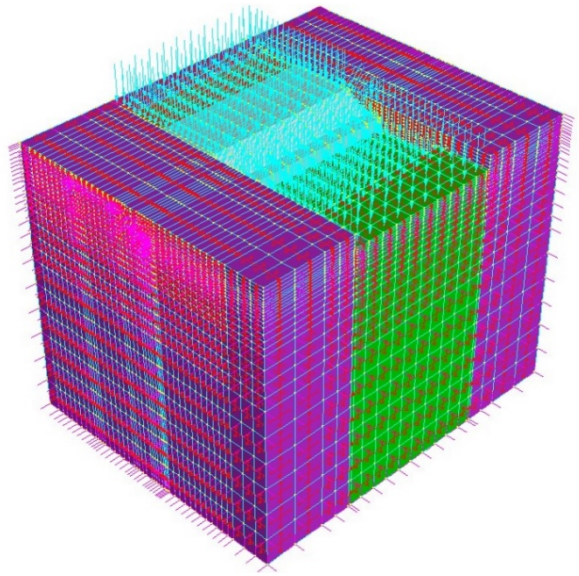

Figure 4. Constitutive floodway model with medium mesh size.

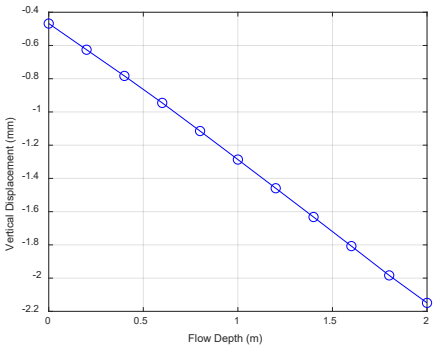

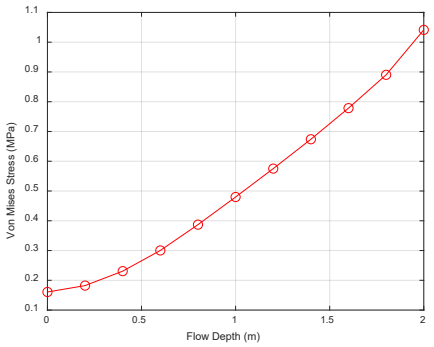

(a) **(b)**

Figure 5. (a) vertical displacement and (b) Von Mises stress for changes in flow depth.

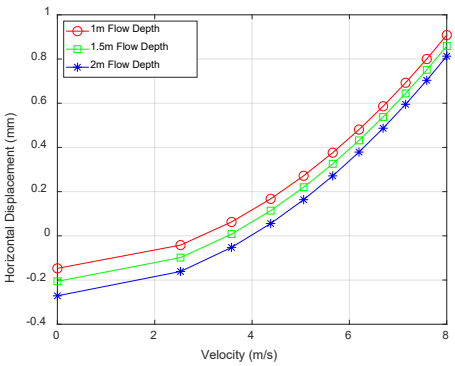

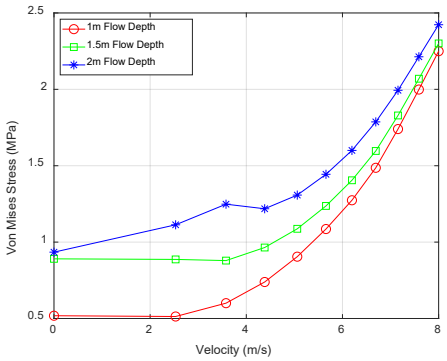

(a) **(b)**

Figure 6. (a) horizontal displacement and (b) Von Mises stress for boulder impact.

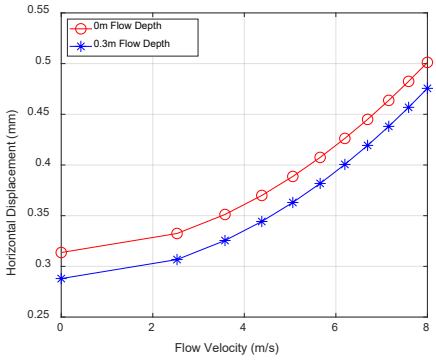

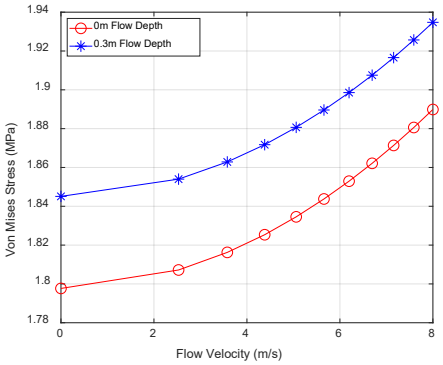

(a) **(b)**

Figure 7. (a) horizontal displacement and (b) Von Mises stress for debris, vehicular and hydrostatic loadings.

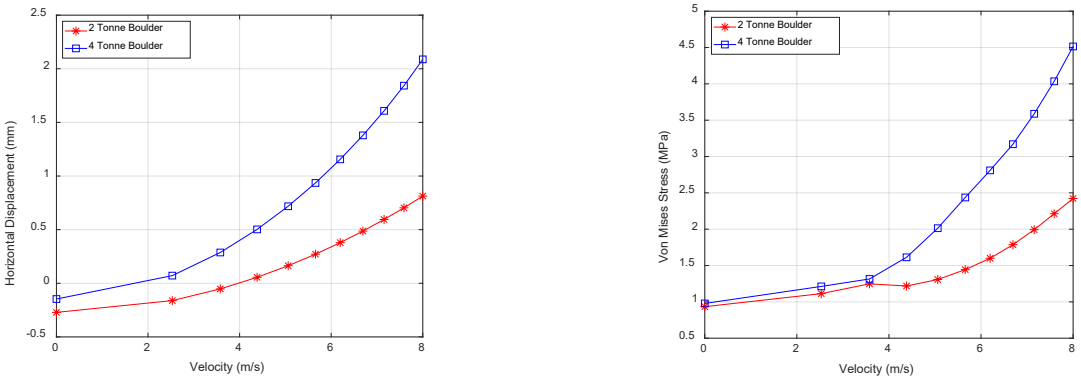

(a) **(b)**

Figure 8. (a) horizontal displacement and (b) Von Mises stress for 2 and 4-tonne boulder impacts.

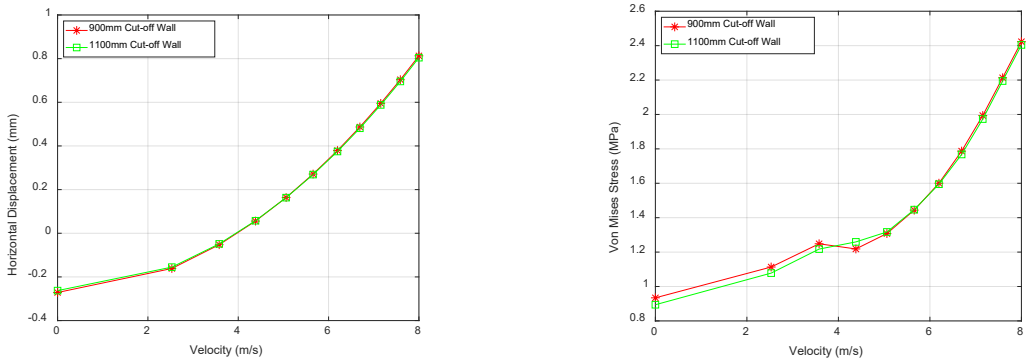

(a) **(b)**

Figure 9. (a) horizontal displacement and (b) Von Mises stress for different cut-off wall configurations.

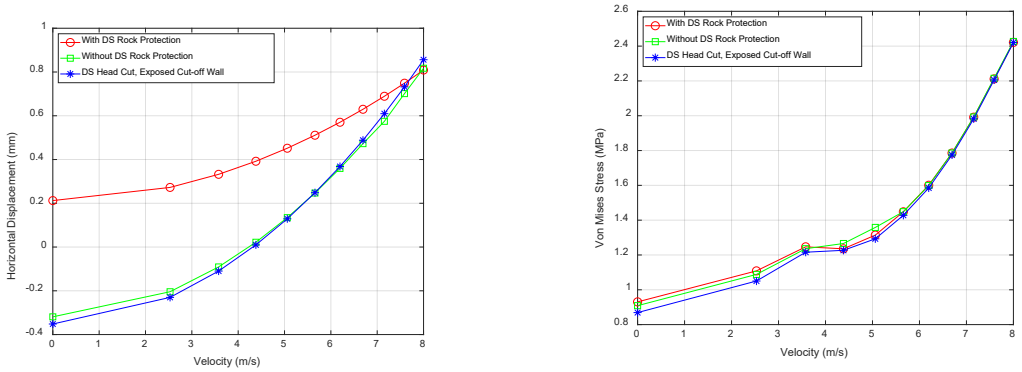

(a) **(b)**

Figure 10. (a) horizontal displacement and (b) Von Mises stress for different downstream rock protection extents.

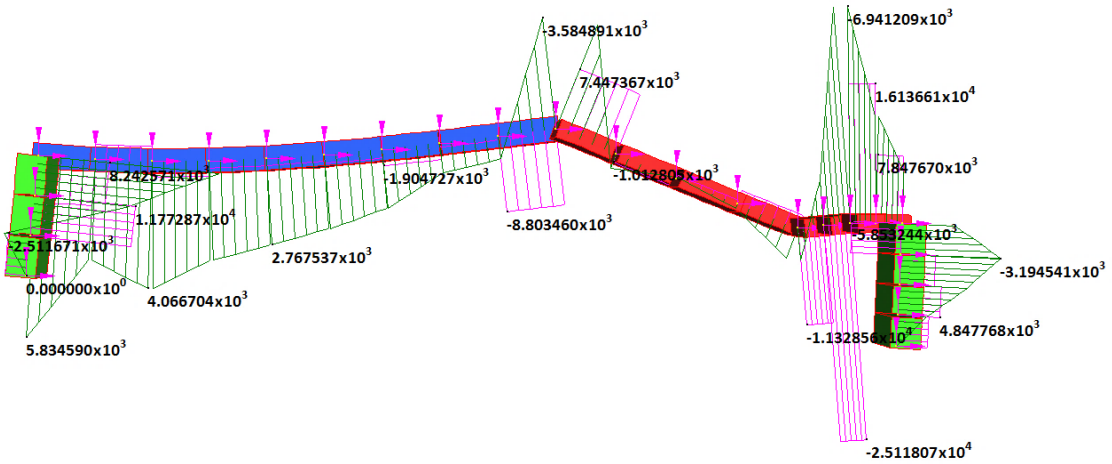

Figure 11. Typical 2D beam bending moment and shear force diagram.

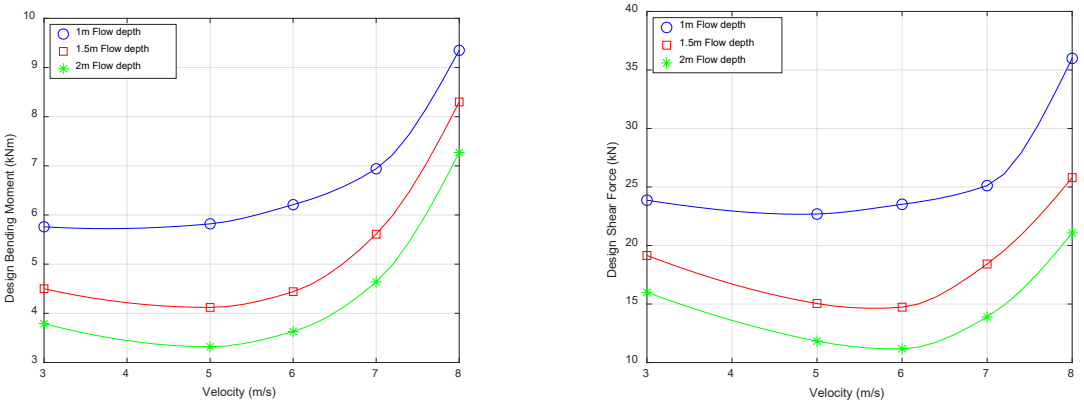

(a) **(b)**

Figure 12. (a) design bending moment and (b) design shear force design charts for soil type 1.

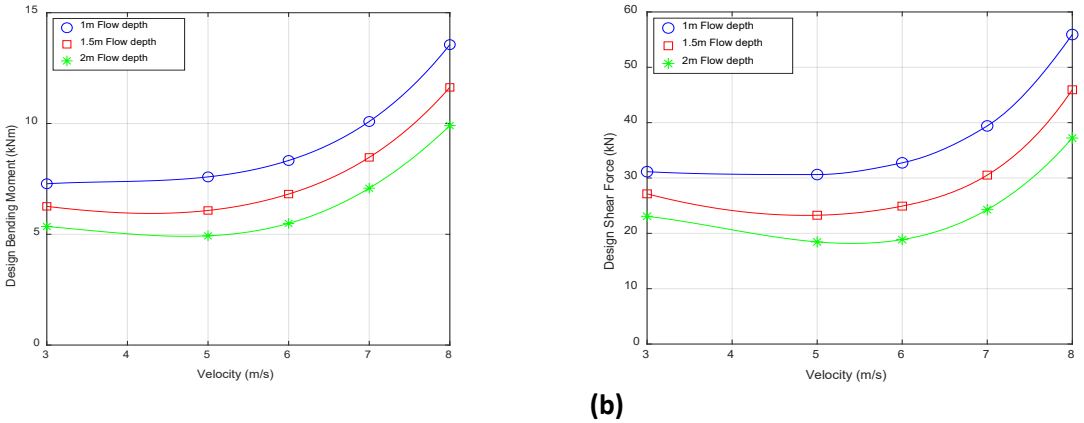

(a) **(b)**

Figure 13. (a) design bending moment and (b) design shear force design charts for soil type 2.

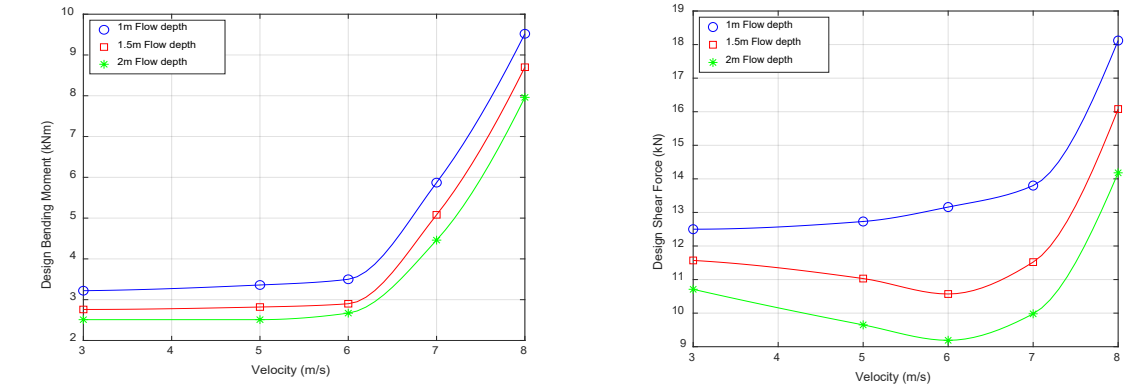

(a) **(b)**

Figure 14. (a) design bending moment and (b) design shear force design charts for soil type 3.

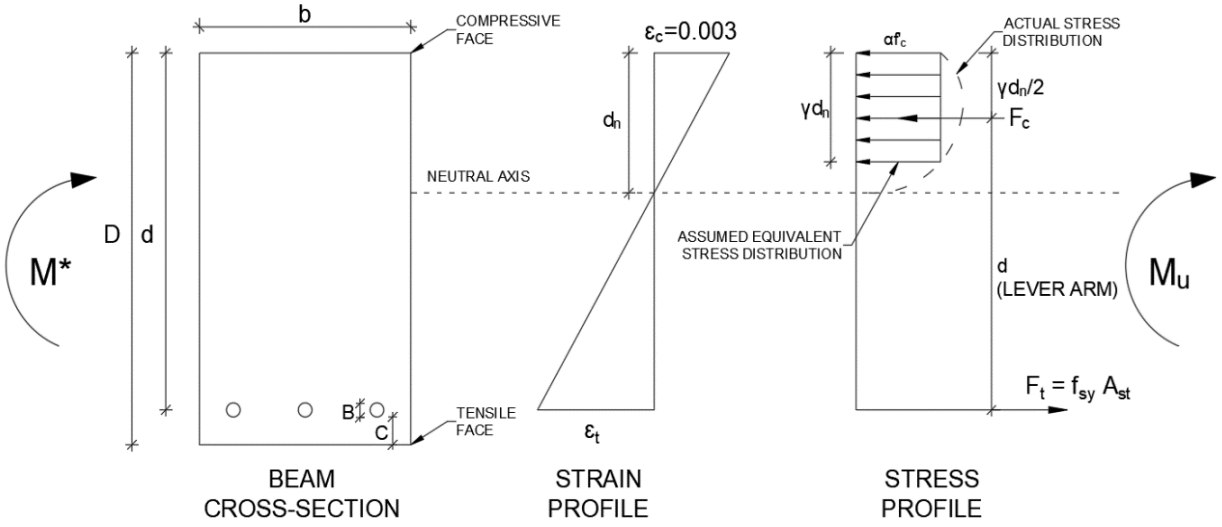

Figure 15. Equivalent concrete stress block for cut-off wall.

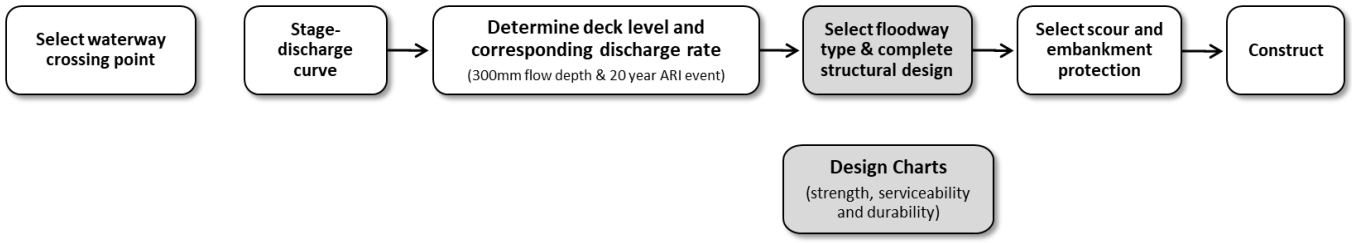

Figure 16. Integrated floodway design process.

Table 1. Mechanical properties of materials used to define the floodway.

Material	Modulus (MPa)	Poisson ratio	Density (kg/m^3)	Cohesion (MPa)	Friction angle (degrees)
Concrete	31,000	0.2	2,400	N/A	N/A
Rock (Obrzud and Truty 2018)	100	0.3	1,400	1.0	30
Natural subgrade (95% MDD)	150	0.3	1,900	0.1	30
Gravel sub base	200	0.3	2,000	0.1	35
Soil 1: Silty Sand	40	0.3	1,700	0.01	25
Soil 2: Sandy Soil	30	0.25	1,800	0.075	34
Soil 3: Clay Soil	100	0.3	1,900	0.01	20

Table 2. Dx displacement versus load for with and without contact (μ = 0.55).

Horizontal Load (MPa)	0.0197	0.0400	0.0575	0.0582	0.0590	0.0625
Max Dx (mm) without Contact	0.720	0.830	0.940	0.945	0.951	0.970
Max Dx (mm) With Contact	0.707	0.830	2.180	5.650	Not converged	Not converged

Table 3. Mechanical properties for insitu adjoining soils.

Material Type	E (MPa)	ν	ρ (kg/m^3)	c' (MPa)	ϕ (°)	K0	e
Soil 1: Silty Sand	40	0.3	1,700	0.01	25	0.426	0.4
Soil 2: Sandy Soil	30	0.25	1,800	0.075	34	0.44	0.3
Soil 3: Clay Soil	100	0.3	1,900	0.01	20	0.658	0.15